

Effect of Random Packing on Stress Relaxation in Foam

Stephen A. Langer

Mathematical and Computational Sciences Division, NIST, Gaithersburg, Maryland 20899

Andrea J. Liu*

Department of Chemistry and Biochemistry, University of California, Los Angeles, California 90095

Received: April 11, 1997[⊗]

Numerical simulations are conducted to examine the effect of randomness in the bubble packing on the local elastic properties of a foam. We find that the response to a small-amplitude strain is spatially inhomogeneous: there are regions (of several bubbles) where bubbles shift their positions in order to prevent distortion. These regions respond differently when sheared in different directions, showing that the regions are elastically anisotropic. This work verifies assumptions made in an earlier, coarse-grained model.

A liquid foam is a concentrated dispersion of gas or liquid bubbles suspended in an immiscible liquid and stabilized by a surfactant. In a foam, the volume fraction of the bubbles exceeds random close-packing; this is possible because the randomly-packed bubbles are deformable. As a result, a foam is highly elastic since the energy required to change the relative positions of bubbles is large compared to the thermal energy. However, a foam can also dissipate energy; this makes it viscoelastic. The disorder in the bubble packing structure causes a foam to resemble a glass more than a crystalline solid and affects the viscoelastic response. For example, a macroscopic shear strain does not produce an affine deformation of the structure, because some bubbles shift while others distort under the applied strain. This leads to more dissipation and less storage of energy than in a periodic packing of bubbles. Recently, Liu et al.¹ proposed a simple, coarse-grained model based on this idea and predicted that the complex dynamic shear modulus should contain an anomalous contribution that varies as the square root of frequency. The predicted behavior was observed over six decades of frequency in a randomly-packed, monodisperse liquid–liquid foam (emulsion).¹ This success is encouraging, but the model is highly speculative because it is based on three important assumptions that are not obviously true. First, Liu et al. assume that some bubbles shift while others distort under a small-amplitude applied strain. Second, they assume that the bubbles that shift are spatially correlated into “weak regions”. Finally, they assume that these weak regions are anisotropic in their elastic properties. That is, bubbles can shift in a local weak region, but only parallel to a certain plane whose orientation varies randomly from weak region to weak region. In addition to being speculative, the coarse-grained model has the drawback of being divorced from a microscopic description of the foam in that it replaces individual bubbles with regions of several bubbles that are described only in terms of an elastic free energy. A recent coarse-grained model introduced by Sollich and co-workers² follows a similar procedure by replacing individual bubbles with regions of bubbles that are characterized in terms of a yield strain and yield energy.

In this paper, we test the assumptions of the coarse-grained model of Liu and co-workers and establish the connection between the model and the bubble packing, using numerical

simulations of a simple bubble-scale model of foams.^{3,4} Unlike Liu et al.,¹ we do not study the response of the system to a small-amplitude oscillatory shear strain but rather the response to a small-amplitude step strain. The coarse-grained model can be applied to either an oscillatory strain or a step strain in the linear regime, and it turns out to be much easier to test the assumptions of the coarse-grained model with a step strain. Our results support the assumptions of the model: we find that there are indeed bubbles that shift to avoid distortion and that these bubbles are spatially correlated into weak regions that are anisotropic. We are less successful in trying to predict, for a given bubble packing, where the weak regions are.

All of our simulations are conducted on a model developed by Durian^{3,4} which focuses on entire bubbles as the building blocks of the foam and considers their motion in response to interactions. Two types of interactions between bubbles are considered; both are approximated as pairwise additive^{5,6} and are expressed in terms of the center of mass positions, $\{\mathbf{r}_i\}$ and the radii, $\{R_i\}$, of the bubbles. The first interaction is purely repulsive and originates physically in the energy cost to distort bubbles. If the distance between the centers of two bubbles is greater than the sum of their radii (if they do not overlap), then the two bubbles are assumed not to interact. If the distance between their centers is smaller than the sum of their radii, however, the bubbles will deform to avoid overlap. This gives rise to a repulsive central force that is approximated as harmonic.^{5,7} Thus, the deformation energy is replaced by the elastic energy of a spring connecting two overlapping bubbles. We assume the spring force to be derived from the Laplace pressure of the bubbles and to be proportional to $1/R_i$. The second interaction considered arises from dissipation in the liquid film between moving bubbles. The resulting force is assumed to be proportional to the velocity difference of neighboring bubbles; this is the simplest form for a viscous drag. The equation of motion for bubble i is then³

$$\mathbf{v}_i = \langle \mathbf{v}_j \rangle + \frac{F_0}{b} \left\langle \left[\frac{1}{|\mathbf{r}_i - \mathbf{r}_j|} - \frac{1}{R_i + R_j} \right] (\mathbf{r}_i - \mathbf{r}_j) \right\rangle + \frac{\mathbf{F}_i^{\text{app}}}{b} \quad (1)$$

where the angular brackets represent averages over those bubbles j that overlap bubble i (that is, $|\mathbf{r}_i - \mathbf{r}_j| < R_i + R_j$). The characteristic force, F_0 , is set by the surface tension and the average bubble radius, and b is the viscous drag coefficient. The bubbles can also move in response to an external force,

* Corresponding author.

[⊗] Abstract published in *Advance ACS Abstracts*, October 1, 1997.

F^{app}. In the simulation, we set the average bubble radius $\langle R \rangle$ to unity. There is also a characteristic relaxation time scale defined by $\tau = b\langle R \rangle / F_0$, which we also set to unity.⁸ Equation 1 can be written as a matrix equation that must be solved for all the bubble velocities as functions of the bubble positions. Our simulations are conducted in two dimensions on polydisperse bubbles that occupy an area fraction of 95% and are drawn from a flat bubble-size distribution that ranges from 0.2 to 1.8 times the average bubble radius.

Our analysis is based on a simple numerical experiment that starts with an equilibrated system with the bubbles at positions $\{\mathbf{r}_i^{\text{eq}}\}$. At time $t = 0$, we apply a small-amplitude affine step strain γ , so that at time $t = 0^+$ the positions of the bubbles, $\{\mathbf{r}_i^0\}$, are shifted by $\gamma y_i \hat{\mathbf{x}}$ with respect to $\{\mathbf{r}_i^{\text{eq}}\}$, where y_i is the y component of the position of bubble i . We then allow the system to relax to a final set of positions, $\{\mathbf{r}_i^\infty\}$. In order to test the assumptions of the coarse-grained model, we must quantify the deviation from an affine deformation. We have developed three different ways of quantifying the deviation. The first two measure the shift of the bubble positions as the system relaxes from the affine deformation (i.e., they measure “slip”), and the third quantity measures the change in the elastic energy stored in the harmonic springs connecting overlapping bubbles. We call the first quantity \mathbf{S}_i^a . It measures the shift of the relaxed bubble positions from their initial positions relative to the affine deformation:

$$\mathbf{S}_i^a = \frac{\mathbf{r}_i^\infty - \mathbf{r}_i^{\text{eq}}}{\mathbf{r}_i^0 - \mathbf{r}_i^{\text{eq}}} - \hat{\mathbf{x}} \quad (2)$$

If the deformation were affine, then the first term on the left-hand side of eq 2 would reduce to $\hat{\mathbf{x}}$. We have therefore subtracted $\hat{\mathbf{x}}$ to ensure that \mathbf{S}_i^a vanishes when the deformation is affine.

A second definition of slip considers the shift of the position of bubble i relative to the average shift of the position of its neighbors during the relaxation process.

$$\mathbf{S}_i^b = \mathbf{r}_i^\infty - \mathbf{r}_i^0 - \langle \mathbf{r}_i^\infty - \mathbf{r}_j^0 \rangle \quad (3)$$

The average runs over overlapping neighboring bubbles. This quantity also vanishes when the deformation is affine, because $\mathbf{r}_i^\infty = \mathbf{r}_i^0$ for all bubbles in that case.

Finally, we keep track of the elastic energy, E_{ij} , stored in the spring between two overlapping neighboring bubbles i and j ; this represents the deformation energy due to the interaction between the two bubbles. We define E_{ij}^0 to be the elastic energy of the spring at time $t = 0^+$ after the applied affine step strain and E_{ij}^∞ to be the elastic energy of the spring when the system has reequilibrated. The total elastic energy, $E = \frac{1}{2} \sum_{ij} E_{ij}$, can be monitored as the system relaxes after the deformation is imposed. E decreases as the bubbles shift and dissipate energy. If we examine the energies of individual springs, however, we find that some springs are less compressed than if the deformation were affine ($E_{ij}^\infty < E_{ij}^0$), and other springs are more compressed ($E_{ij}^\infty > E_{ij}^0$). We therefore study the quantity $\delta E_{ij} = E_{ij}^\infty - E_{ij}^0$, which is negative for springs associated with bubbles that shift to avoid distortion.

We can now address the three assumptions underlying the coarse-grained model in terms of \mathbf{S}_i^a , \mathbf{S}_i^b , and δE_{ij} .

Assumption 1: Some Bubbles Shift While Others Distort under an Applied Strain. Durian⁴ has found nonaffine deformation by plotting the vector quantity $\mathbf{S}_i^a + \hat{\mathbf{x}}$ (see eq 2)

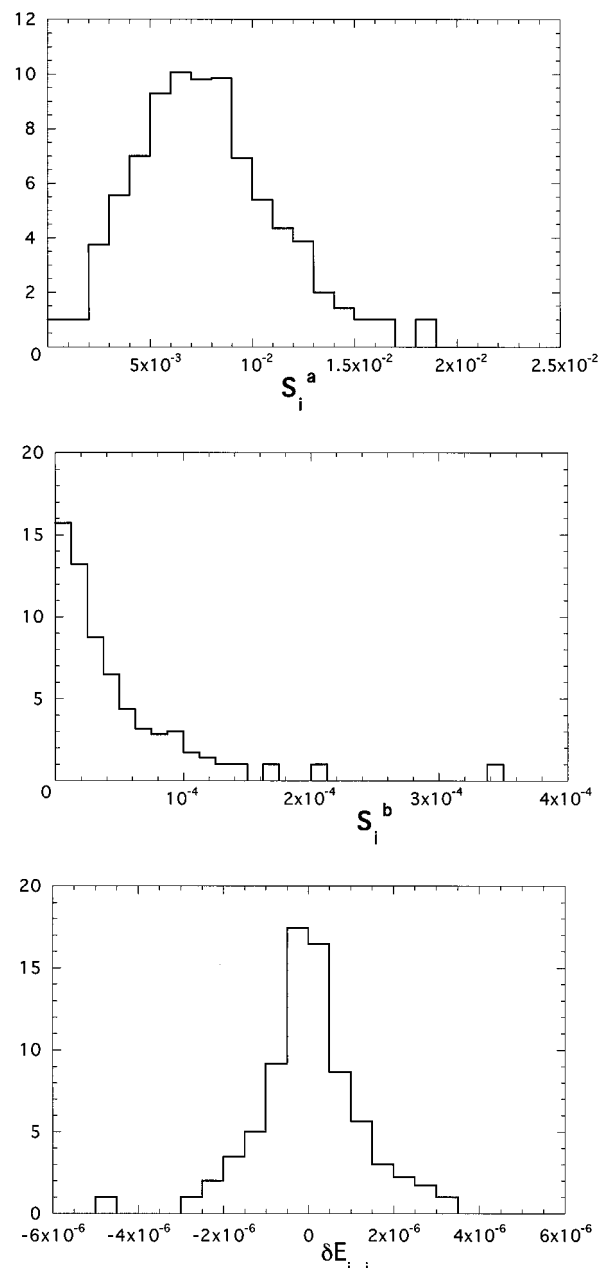


Figure 1. Histograms for a given sample of (a, top) the magnitude of the slip defined in eq 2, \mathbf{S}_i^a , (b, middle) the magnitude of slip defined in eq 3, \mathbf{S}_i^b , and (c, bottom) the change in bond energy during relaxation following step strain, δE_{ij} . In all three cases, we have taken the square root of the number of bubbles in each bin (the y-axis) to enhance the visibility of the tails of the distributions. For an affine deformation, \mathbf{S}_i^a , \mathbf{S}_i^b , and δE_{ij} would be zero for all bubbles.

and showing that the resulting vectors are not all of the same magnitude and direction. Lacasse and co-workers⁵ also plotted this quantity and found deviations from affine behavior for three-dimensional, random packings of monodisperse bubbles. Here we examine the same behavior, but in terms of \mathbf{S}_i^a , \mathbf{S}_i^b , and δE_{ij} . If the deformation were affine, then we would find $\mathbf{S}_i^a = 0$, $\mathbf{S}_i^b = 0$, and $\delta E_{ij} = 0$ for all bubbles. The fact that we observe that $\mathbf{S}_i^a \equiv |\mathbf{S}_i^a|$ and $\mathbf{S}_i^b \equiv |\mathbf{S}_i^b|$ are nonzero and that δE_{ij} is negative for some bubbles is proof that assumption 1 is correct. This can be seen from Figure 1, where we have constructed histograms for a 25×25 bubble sample subjected to a step strain $\gamma = 0.001$, which is well within the linear regime. Figure 1a is a histogram of \mathbf{S}_i^a , Figure 1b is a histogram of \mathbf{S}_i^b , and Figure 1c is a histogram of δE_{ij} . Note that most of the bubbles

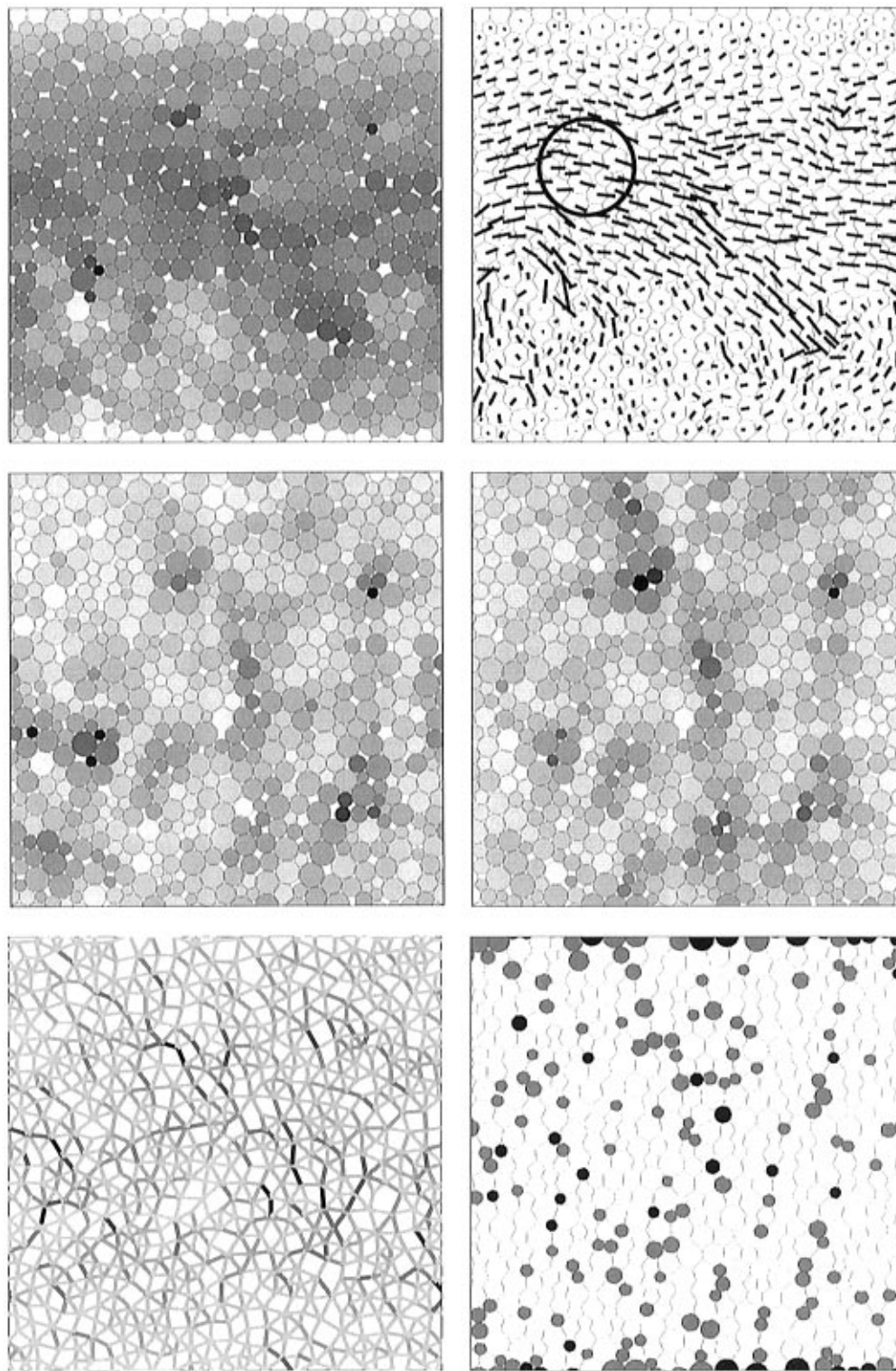


Figure 2. Gray-scale plots showing (a, left top) the magnitude of slip for each bubble i , S_i^a , and (b, left middle) the magnitude of slip, S_i^b . The gray scale does not correspond to the full range of the data, but has been adjusted to maximize contrast; darker shades correspond to larger values of slip. (c, left bottom) The change in bond energy for each bond ij , δE_{ij} , with darker shades corresponding to more negative values of δE_{ij} . There are definite correlations between the dark regions in the three figures, showing that S_i^a , S_i^b , and δE_{ij} are all reasonable ways of quantifying weak regions. (d, right top) A vector plot of the slip S_i^a defined in eq 2. For each bubble i , the direction of S_i^a is shown by a line segment that starts at the center of the bubble. The magnitude S_i^a is proportional to the length of the line segment. The circled region contains a number of bubbles that have similar values of S_i^a . (e, right middle) A gray-scale plot of the slip S_i^b for the same sample shown in (a–d), subjected to a step strain applied in the $-\hat{y}$ direction. (a–d) all correspond to a step strain applied in the \hat{x} direction. The fact that (b) is different from (e) shows that the system is locally anisotropic, even though it is isotropic on average. (f, right bottom) The number of overlapping neighbors, Z , is shown for the same sample as in (a–e). The median value of Z is 6. Bubbles with $Z = 3$ are black, those with $Z = 4$ are gray, and those with $Z > 4$ are white. A comparison with (b) and (e) shows that all weak regions contain low- Z bubbles, but not all low- Z bubbles belong to weak regions.

show small deviations from affine behavior. However, there are tails in the distributions in Figure 1, a and b, toward large

values of slip; bubbles in these tails correspond to those that have shifted the most. Similarly, there is a tail toward negative

values of δE_{ij} in Figure 1c; springs in this tail correspond to those that have lowered their energy the most.

Assumption 2: Bubbles That Shift To Avoid Distortion are Spatially Correlated into "Weak Regions". Figure 2, a and b, shows that bubbles with large values of slip, S_i^a or S_i^b , are indeed spatially correlated. We have plotted S_i^a and S_i^b on a gray scale for each bubble (darker bubbles have larger values of slip), for a 25×25 bubble system subjected to a step strain of $\gamma = 0.001$. It is clear from Figure 2a,b that dark bubbles tend to be surrounded by dark bubbles. Clusters of dark bubbles correspond to weak regions. Note that the two definitions of slip (see eqs 2 and 3) yield different results. However, there are definite correlations; bubbles that are dark in Figure 2a tend also to be dark in Figure 2b. This is reassuring, because both definitions are valid ways of quantifying the deviation from an affine deformation. The main difference between the two definitions is illustrated in Figure 2d, where we have plotted S_i^a with lines that start at the centers of the bubbles and point in the direction of the vectors. The lengths of the lines are proportional to the magnitude S_i^a . The circled region in Figure 2d corresponds to a cluster of bubbles that have all shifted by roughly the same amount in the same directions. Thus, the entire cluster moved, but bubbles within the cluster have maintained the same packing. If we examine the same region in Figure 2a, we see that S_i^a is fairly large there. On the other hand, in Figure 2b, the values of S_i^b are small there, since the bubbles are all shifting together. Since we are only interested in shifts that affect the deformation energies of bubbles, it is more appropriate to use the second definition of slip, S_i^b , in eq 3. The remainder of this paper will therefore focus only on S_i^b and δE_{ij} to quantify deviations from affine behavior.

The tails of the histograms in Figure 1b, c show that there are bubbles that slip and springs that lower their energy during the relaxation process. We expect that bubbles slip in order to lower the elastic interaction energy with neighboring bubbles, so S_i^b should be large and δE_{ij} should be negative in the same regions of the sample. Figure 2c shows that this is in fact the case. Here, we have plotted the bonds between overlapping bubbles, that the line segments connect the centers of interacting bubbles. The bonds are shaded on a gray scale according to the value of δE_{ij} . Thus, large and negative values of δE_{ij} are represented by black bonds and positive values are represented by light gray bonds. A comparison of Figure 2b Figure 2c shows that regions that contain dark bubbles in Figure 2b also contain dark bonds in Figure 2c.

Assumption 3: Weak Regions Are Anisotropic in Their Elastic Properties. To test for anisotropy, we shear the same samples in two different directions. In Figure 2a–d, we have applied a step strain of $\gamma = 0.001$ in the \hat{x} direction. We have applied the strain by moving the top edge to the right, holding the bottom edge fixed. There is a periodic boundary condition the \hat{x} direction. In Figure 2e, we have started with the same sample, but we have applied a step strain of $\gamma = 0.001$ in the $-\hat{y}$ direction. We have applied the strain by moving the right edge downwards, holding the left edge fixed. This time, there is a periodic boundary condition in the \hat{y} direction. The results for S_i^b are shown on a gray scale in Figure 2e. Figure 2, b and e, therefore shows the effects of applying step strain in the \hat{x} and $-\hat{y}$ directions, respectively. If the weak regions were isotropic, then the gray scale pictures in parts b and e would be identical since we have plotted S_i^b in both cases with the same gray scale. There are indeed definite correlations between parts b and e. However, there are also important differences. There are regions that are dark in Figure 2 but not in Figure 2e, but

these are close to the boundaries and may be affected by the different boundary conditions in the two cases. More significantly, several of the dark regions in Figure 2b are less dark in Figure 2e, and vice versa. This supports the assumption that the regions are anisotropic.

Our results support the assumption that anisotropic weak regions exist, but this is not enough to clarify fully the connection between the coarse-grained model and the microscopic model of bubble packing. Ideally, we should be able to predict, for a given bubble packing, the location, extent, and orientation of weak regions. This turns out to be quite difficult. One possibility is bubbles that are poorly-packed tend to slip more. To test this, we have examined the coordination number, Z_i , i.e. the number of overlapping neighbors of bubble i . Figure 2f shows the bubbles that have the fewest neighbors; black bubbles have three overlapping neighbors and gray bubbles have four. Bubbles with more than four overlapping neighbors are white. A comparison of Figure 2f and Figure 2b,e shows that each weak region does contain at least one low- Z bubble, and several weak regions contain clusters of such bubbles. However, there are many low- Z bubbles, and clusters of low- Z bubbles, that do not lie in weak regions, so we cannot use this criterion to predict the location of weak regions.

One natural question is whether we observe the stress relaxation predicted by the coarse-grained model. According to the model, in response to a step strain the stress should decay with time as

$$\sigma_{xy}(t) \approx \sigma_\infty + At^{-1/2} \quad (4)$$

at long times t . The time-dependent modulus, $G(t)$, is the ratio of the stress to the strain, and therefore has the same form. Thus, the theory predicts that $\delta G(t) = G(t) - G_\infty$ should decay as the inverse square root of time. The origin of the power-law decay lies in the distribution of orientations of anisotropic weak regions relative to the shear direction. The stress in a given region relaxes exponentially with a rate that depends on the orientation of the region. For a system with many weak regions, there is a broad distribution of stress relaxation times that leads directly to the predicted power-law stress relaxation. In the simulations, however, we always find that the stress relaxation is exponential for sufficiently long times. Similar results for elastic energy relaxation were obtained earlier by Durian.³ The exponential decay could be a consequence of small sample size: there are simply not enough weak regions in our samples, so there is not a broad distribution of relaxation rates. To test this hypothesis, we have examined the stress relaxation rate as a function of system size. If the problem lies in our small sample sizes, then the stress relaxation rate should increase with system size. Over the range of system sizes studied (up to 25×25), however, we find that the variations in the relaxation rate from sample to sample overwhelm any dependence on system size.

In summary, we find that randomness has a strong effect on the linear shear response of a foam. In particular, random packing leads to correlated spatial inhomogeneities in the foam and the response of the foam, while isotropic over the entire sample, is anisotropic at the local level, on the scale of several bubbles. The coarse-grained model of Liu et al.¹ has the advantage of being analytically tractable but does not provide a description of a foam at the microscopic length scale, namely the size of a bubble. Our numerical simulations, which are conducted on a bubble-scale model, provide the microscopic insight that is lacking in the coarse-grained model. However, more work is required to fully understand the connection between the microscopic bubble packing and the local elastic properties of a foam.

Acknowledgment. This paper is dedicated to Daniel Kivelson on the occasion of his 67th birthday. We thank Douglas J. Durian for many instructive discussions, and gratefully acknowledge support from NSF grant CHE-9624090.

References and Notes

- (1) Liu, A. J.; Ramaswamy, S.; Mason, T. G.; Gang, H.; Weitz, D. A. *Phys. Rev. Lett.* **1996**, 76, 3017.
- (2) Sollich, P.; Lequeux, F.; Hébraud, P.; Cates, M. E. *Phys. Rev. Lett.* **1997**, 78, 2020.
- (3) Durian, D. J. *Phys. Rev. Lett.* **1995**, 75, 4780.
- (4) Durian, D. J. *Phys. Rev. E* **1997**, 55, 1739.
- (5) In fact, the interactions are not pairwise additive. See: Lacasse, M. D.; Grest, G. S.; Levine, D.; Mason, T. G.; Weitz, D. A. *Phys. Rev. Lett.* **1996**, 76, 3448. This affects the magnitude of the elastic modulus, but should not affect the qualitative features that we are exploring.
- (6) Lacasse, M. D.; Grest, G. S.; Levine, D. *Phys. Rev. E* **1996**, 54, 5436.
- (7) Morse, D. C.; Witten, T. A. *Europhys. Lett.* **1993**, 22, 549.
- (8) Note that we have implemented the viscous interaction in a different way from Durian, who replaced the sum over neighbors j in the first term on the right-hand side of eq 1 with the velocity given by the macroscopic average velocity profile at that point. This difference cannot affect static or quasistatic properties but may affect dynamical quantities such as the rate of stress relaxation.